Latin American Journal of Solids and Structures
www.lajss.org

A New Fifth-Order Shear and Normal Deformation Theory for Static Bending and Elastic Buckling of P-FGM Beams

Abstract

A new fifth-order shear and normal deformation theory (FOSNDT) is developed for the static bending and elastic buckling analysis of functionally graded beams. The properties of functionally graded material are assumed to vary through the thickness direction according to power-law distribution (P-FGM). The most important feature of the present theory is that it includes the effects of transverse shear and normal deformations. Axial and transverse displacements involve polynomial shape functions to include the effects of transverse shear and normal deformations. A polynomial shape function expanded up to fifth-order in terms of the thickness coordinate is used to account for the effects of transverse shear and normal deformations. The kinematics of the present theory is based on six independent field variables. The theory satisfies the traction free boundary conditions at top and bottom surfaces of the beam without using problem dependent shear correction factor. The closed-form solutions of simply supported FG beams are obtained using Navier's solution procedure and non-dimensional results are compared with those obtained by using classical beam theory, first order shear deformation theory and other higher order shear deformation theories. It is concluded that the present theory is accurate and efficient in predicting the bending and buckling responses of functionally graded beams.

Keywords

Functionally graded beam, transverse shear deformation, transverse normal deformation, bending, buckling.

S. M. Ghumare [a, *]
A. S. Sayyad [b]

[a] Research Scholar, Department of Civil Engineering, SRES's Sanjivani College of Engineering, Savitribai Phule Pune University, Kopargaon-423603, Maharashtra, India.
E-mail: smghumare@rediffmail.com
[b] Professor, Department of Civil Engineering, SRES's Sanjivani College of Engineering, Savitribai Phule Pune University, Kopargaon-423603, Maharashtra, India.
E-mail: attu_sayyad@yahoo.co.in

* Corresponding author

http://dx.doi.org/10.1590/1679-78253972

Received 26.04.2017
In revised form 13.06.2017
Accepted 03.07.2017
Available online 10.07.2017

1 INTRODUCTION

Today great emphasis is being placed on developing new materials or material systems tailored for specific applications. Currently the main focus of the researcher is to develop new composite

materials due to enormous benefits like improvements in material performance, ability to support optimized structural designs, continued lowering of manufacturing costs, and the ability to perform reliably in service. The traditional composite material is incapable to employ under the high-temperature environments and may fail due to delamination or stress concentration. A functionally graded material (FGM) is a novel class of material having unique characteristics and can be used alternatively to overcome the delamination failure that usually occurs in laminated composites. FGM have received major attention as a heat-shielding advanced structural material in various engineering applications like automobile, aircraft, aerospace projects and defense industry.Functionally graded materials (FGMs) are those in which the volume fraction of two or more materials is varied continuously as a function of position along certain directions of the structure (normally in thickness direction). The FG materials are generally ceramic and metal constituents. The ceramic constituent provides high-temperature resistance due to its low thermal conductivity; whereas the ductile metal constituent prevents fracture caused by stresses due to the high temperature gradient in a very short span of time and provides stronger mechanical performance.

Functionally graded material is the first time developed in 1984 by a group of material scientists in Japan during a space plane project in the form of thermal barrier material which can withstand a huge temperature fluctuation across a very thin cross-section. Development in FG material and its applications can be found in the literature by Koizumi (1993, 1997), Muller et al. (2003) and Birman and Byrd (2006, 2007). Rasheedat et al. (2012) discussed the various processing techniques and interdisciplinary applications of FGM. The more information on beams and plates made of FGM is found in Jha et al. (2013) and Swaminathan et al. (2014).

The well-known elasticity solution for simply supported functionally gradient beams subjected to sinusoidal loading was developed by Sankar (2001). Material properties are assumed to vary according to an exponential law. Further, few more researchers have presented research on elasticity solutions for functionally graded beams Zhong and Yu (2007), Daouadji et al. (2013), Chu et al. (2015). 2D elasticity solutions for thick functionally graded beams are analytically very difficult and computationally cumbersome. Therefore, several analytical and numerical methods have been proposed by researchers to analyze the FG beams accurately using approximate lower and higher order shear deformation theories.

The classical beam theory (CBT) developed by Bernoulli- Euler is the simplest beam theory for the analysis of thin beams. But, since the shear deformation effect is neglected in this theory, it is not suitable for the analysis of thick FG beams. When the FG beam is thick, the classical beam theory underestimates displacements and stresses. In 1921, Timoshenko has developed a theory in which the first order variation of axial displacement is assumed. Therefore, it is called as the first order shear deformation theory (FSDT) or Timoshenko beam theory (TBT). The FSDT does not satisfy the zero transverse shear stress conditions on the top and bottom surfaces of the beam. This theory also required a shear correction factor to properly account the strain energy due to shear deformation effect. Therefore, to predict the accurate bending response of thick FG beams, higher-order shear deformation theories have been proposed by many researchers. The detailed review of these theories along with their displacement model is recently presented by Sayyad and Ghugal (2015,2017a).

Reddy (1984) developed well known third order parabolic shear deformation theory for the analysis of composite beams, plates and shells. Benatta et al. (2008) presented a static analysis of functionally graded shear deformable beams considering three point bending. Li et al. (2010) developed the higher order shear deformation theory for bending of functionally graded beams and proved that the displacements and stresses are depend on the gradient variation of material properties. Pendhari et al. (2010) developed a simple mixed semi analytical model for 2D stress analysis of functionally graded beams subjected to transverse load and compared the results with those obtained by using Navier's closed form solution. Giunta et al. (2010, 2011) proposed several higher order refined theories based on the Carrera's unified formulation for the analysis of functionally graded beams. Thai and Vo (2012) studied static bending and free vibration of functionally graded beams based on various higher-order shear deformation beam theories and Navier's solution technique.Li and Batra (2013) applied CBT and FSDT for the buckling analysis of functionally graded beams of various boundary conditions. Nguyen et al. (2013) presented bending and free vibration of functionally graded beams using FSDT. Vo et al. (2014) presented static and free vibration analysis of functionally graded beams using refined shear deformation theory. Bourada et al. (2015) developed a new trigonometric shear and normal deformation theory for bending and free vibration of functionally graded beams. Simsek (2016) presented buckling of bi-directional functionally graded Timoshenko beams with different boundary conditions using Ritz method. Recently, Sayyad and Ghugal (2017b) developed a unified shear deformation theory for bending of functionally graded plates and beams and obtained closed form solutions using Navier's solution technique.

In the present study, a fifth-order shear and normal deformation theory is developed for the bending and buckling analysis of functionally graded beams subjected to transverse and axial loadings. The most important feature of the present theory is that it includes for the effects of transverse shear and normal deformations. A polynomial shape function expanded up to fifth-order in terms of the thickness coordinate is used to account the effects of transverse shear and normal deformations. The kinematics of the present theory are based on six independent field variables. The theory satisfies the traction free boundary conditions at top and bottom surfaces of the beam without using problem dependent shear correction factor. The closed-form solutions of simply supported FG beams are obtained using Navier's solution procedure and non-dimensional results are compared with those obtained by using classical beam theory, first order shear deformation theory and other higher order shear deformation theories.

2 FORMULATION OF THE PRESENT THEORY

A simply supported FG beam as shown in Fig.1 is considered for the variational formulation and analytical solution. The beam has the length $\boldsymbol{L}$ in x-direction and the overall thickness $\mathbf{h}$ in z-direction. The width of the beam in $\mathbf{y}$-direction is considered as a unity. The origin is assumed at the left end of the beam. The top surface of the beam is made of metal and the bottom surface is made of ceramic.

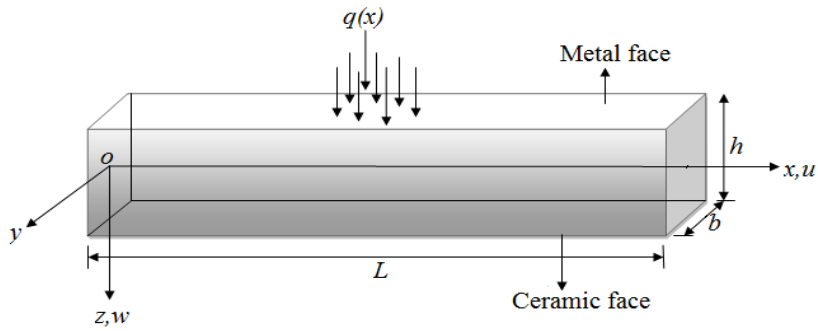

Figure 1: Geometry and coordinates of P-FGM beam under consideration

2.1 Novelty of the Present Theory

The transverse shear and normal deformations play an important role in predicting the accurate structural behaviour of beams and plates made of advanced composite materials. Therefore, any refinements of classical beam theories are generally meaningless, unless the effects of transverse shear and normal strains are both taken into account. This is also discussed by Carrera (2005) and Carrera et al. (2011). In the view of this, the present theory is having following important features.

1) The most important feature of the present theory is that it includes the effects of transverse shear and normal deformations.
2) The axial displacement in the x direction consists of extension, bending and shear components. The axial displacement is expressed in terms of polynomial shape function expanded up to the fifth-order in terms of the thickness coordinate.
3) The transverse displacement is a function of both x and z coordinates. Hence the theory is designated as the fifth-order shear and normal deformation theory.
4) The theory contains six independent unknown variables.
5) The theory enforces the parabolic variation of the transverse shear stress across the thickness of the beam. Thus, the theory obviates the need for the shear correction factor.

2.2 Kinematics

Based on the above features, the displacement field of the present theory is as follows:

$$u(x,z) = u_0(x) - z\frac{dw_0}{dx} + z\left(1 - \frac{4}{3}\frac{z^2}{h^2}\right)\phi_x(x) + z\left(1 - \frac{16}{5}\frac{z^4}{h^4}\right)\psi_x(x)$$
$$w(x,z) = w_0(x) + \left(1 - 4\frac{z^2}{h^2}\right)\phi_z(x) + \left(1 - 16\frac{z^4}{h^4}\right)\psi_z(x) \quad (1)$$

where u and w are the axial and transverse displacements of any point of the beam; u_0 and w_0 are the x-directional and z-directional displacements of a point on the mid-axis of the beam. The present form of transverse displacement gives bending and shear components separately to understand the effect of transverse normal deformations. ϕ_x and ψ_x are the shear slopes associated

with the transverse shear deformation whereas ϕ_z and ψ_z are the shear slopes associated with the transverse normal deformations. Third order and fifth-order polynomial functions are assigned according to the shearing stress distribution through the thickness of the beam in such a way that shear stress vanishes at top and bottom surfaces of the beam.

The nonzero strain components associated with the present theory are obtained using linear theory of elasticity.

$$\begin{aligned}\varepsilon_x &= \varepsilon_x^0 + zk_x^b + f_1(z)\varepsilon_x^1 + f_2(z)\varepsilon_x^2 \\ \varepsilon_z &= f_1''(z)\phi_z + f_2''(z)\psi_z \\ \gamma_{xz} &= f_1'(z)\gamma_{xz}^{s_1} + f_2'(z)\gamma_{xz}^{s_2}\end{aligned} \tag{2}$$

where

$$\varepsilon_x^0 = \frac{\partial u_0}{\partial x},\quad k_x^b = -\frac{\partial^2 w_0}{\partial x^2},\quad \varepsilon_x^1 = \frac{\partial \phi_x}{\partial x},\quad \varepsilon_x^2 = \frac{\partial \psi_x}{\partial x},\quad \gamma_{xz}^{s_1} = \left(\phi_x + \frac{\partial \phi_z}{\partial x}\right),\quad \gamma_{xz}^{s_2} = \left(\psi_x + \frac{\partial \psi_z}{\partial x}\right),$$

$$f_1(z) = z\left[1 - \frac{4}{3}\frac{z^2}{h^2}\right],\quad f_2(z) = z\left[1 - \frac{16}{5}\frac{z^4}{h^4}\right],\quad f_1'(z) = \left[1 - 4\frac{z^2}{h^2}\right],\quad f_2'(z) = \left[1 - 16\frac{z^4}{h^4}\right] \tag{3}$$

$$f_1''(z) = \left[-\frac{8z}{h^2}\right],\quad f_2''(z) = z\left[-\frac{64z^3}{h^4}\right]$$

2.3 Material Gradation and Constitutive Relation

The properties of functionally graded materials vary continuously due to gradually change in the volume fraction of the constituent materials. In the present study, the material properties of FG beam are assumed to vary continuously through the thickness of the beam according to a power law distribution.

$$E(z) = E_m + (E_c - E_m)\left(\frac{1}{2} + \frac{z}{h}\right)^P \tag{4}$$

Where $\boldsymbol{E}$ is the Young's modulus. Subscripts $\boldsymbol{c}$ and $\boldsymbol{m}$ represent the ceramic and metallic constituents respectively. $\boldsymbol{P}$ is the power law index, which governs the volume fraction gradation. The variation of volume fraction through the thickness of a beam is shown in Fig. 2. The value of $\boldsymbol{P}$ is equal to zero represents a fully ceramic phase, whereas infinite $\boldsymbol{P}$ indicates a fully metallic phase. Through thickness distribution of Young's modulus is linear for P=1 and non-linear for P=2, 5 and 10. The poisons ratio is assumed to be constant since the effect of variation of poisons ratio (μ) on the bending response of FG beam is very small.

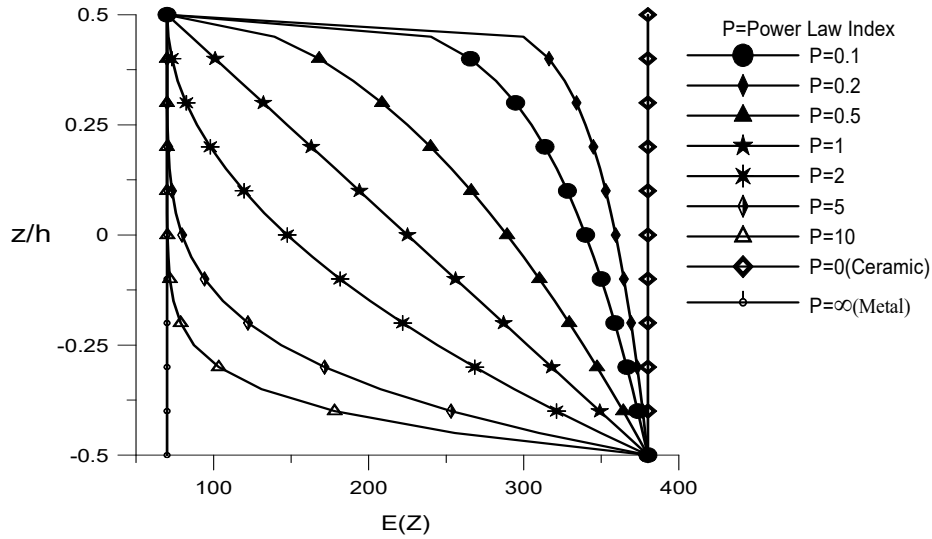

Figure 2: Variation of Young's modulus through the thickness of a P-FGM beam for various values of the power law index.

The linear constitutive relations at a point of the functionally graded beam can be written as

$$\begin{Bmatrix} \sigma_x \\ \sigma_z \\ \tau_{xz} \end{Bmatrix} = \begin{bmatrix} Q_{11}(z) & Q_{13}(z) & 0 \\ Q_{13}(z) & Q_{33}(z) & 0 \\ 0 & 0 & Q_{55}(z) \end{bmatrix} \begin{Bmatrix} \varepsilon_x \\ \varepsilon_z \\ \gamma_{xz} \end{Bmatrix} \tag{5}$$

Where

$$Q_{11}(z) = Q_{33}(z) = \frac{E(z)}{1-\mu^2}, \qquad Q_{13}(z) = \frac{\mu\, E(z)}{1-\mu^2}, \qquad Q_{55}(z) = \frac{E(z)}{2(1+\mu)} \tag{6}$$

2.4 Governing Differential Equations

The six variationally consistent governing differential equations of the present theory are obtained using the principle of virtual displacements.

$$\int_0^L \int_{-h/2}^{h/2} \left(\sigma_x \delta\varepsilon_x + \sigma_z \delta\varepsilon_z + \tau_{xz} \delta\, \gamma_{xz}\right) dz\, dx = \int_0^L \left[q(x)\delta w_0 + N_0 \frac{dw_0}{dx}\frac{d\delta w_0}{dx} \right] dx \tag{7}$$

where the symbol δ denotes the variational operator. Substituting strains from Eq. (2) into the Eq. (7) one can write

$$\begin{aligned} &\int_0^L \Big(N_x \frac{d\delta u_0}{dx} - M_x^b \frac{d^2\delta w_0}{dx^2} + M_x^{S_1} \frac{d\delta\phi_x}{dx} + M_x^{S_2} \frac{d\delta\psi_x}{dx} + Q_z^{S_1}\delta\phi_z + Q_z^{S_2}\delta\psi_z + Q_{xz}^1\delta\phi_x \\ &+ Q_{xz}^1 \frac{d\delta\phi_z}{dx} + Q_{xz}^2\delta\psi_x + Q_{xz}^2 \frac{d\delta\psi_z}{dx} \Big) dx = \int_0^L \left[q(x)\delta w_0 + N_0 \frac{dw_0}{dx}\frac{d\delta w_0}{dx} \right] dx \end{aligned} \tag{8}$$

where

$$\left[N_x, M_x^b, M_x^{S_1}, M_x^{S_2}\right] = \int_{-h/2}^{h/2} \sigma_x \left[1, z, f_1(z), f_2(z)\right] dz,$$
$$\left[Q_{xz}^1, Q_{xz}^2\right] = \int_{-h/2}^{h/2} \tau_{xz} \left[f_1'(z), f_2'(z)\right] dz, \tag{9}$$
$$\left[Q_z^{S_1}, Q_z^{S_2}\right] = \int_{-h/2}^{h/2} \sigma_z \left[f_1''(z), f_2''(z)\right] dz$$

where N_x is the resultant axial force, M_X^b is the resultant moment due to bending, $M_X^{S_1}$ and $M_X^{S_2}$ are the resultant moment due to shear deformation and Q_{xz}^1, Q_{xz}^2, $Q_z^{S_1}, Q_z^{S_2}$ are the resultant shear forces. Integrating Eq. (8) by parts and setting the coefficients of $\delta u_0, \delta w_0, \delta\phi_x, \delta\psi_x, \delta\phi_z, \delta\psi_z$ equals to zero, the following governing differential equations are obtained

$$\delta u_0: \quad \frac{dN_x}{dx} = 0, \qquad \delta w_0: \quad \frac{d^2 M_x^b}{dx^2} + q - N_0 \frac{d^2 w_0}{dx^2} = 0,$$
$$\delta\phi_x: \quad \frac{dM_x^{S_1}}{dx} - Q_{xz}^1 = 0, \quad \delta\psi_x: \quad \frac{dM_x^{S_2}}{dx} - Q_{xz}^2 = 0, \tag{10}$$
$$\delta\phi_z: \quad \frac{dQ_{xz}^1}{dx} - Q_z^{S_1} = 0, \quad \delta\psi_z: \quad \frac{dQ_{xz}^2}{dx} - Q_z^{S_2} = 0$$

The boundary conditions obtained at $x = 0$ and $x = L$ are of the following form

$$\text{Either } N_x = 0 \quad \text{or} \quad u_0 \text{ is prescribed} \tag{11}$$

$$\text{Either } M_x^b = 0 \quad \text{or} \quad \frac{dw_0}{dx} \text{ is prescribed} \tag{12}$$

$$\text{Either } \frac{dM_x^b}{dx} = 0 \quad \text{or} \quad w_b \text{ is prescribed} \tag{13}$$

$$\text{Either } M_x^{S_1} = 0 \quad \text{or} \quad \phi_x \text{ is prescribed} \tag{14}$$

$$\text{Either } M_x^{S_2} = 0 \quad \text{or} \quad \psi_x \text{ is prescribed} \tag{15}$$

$$\text{Either } Q_{xz}^1 = 0 \quad \text{or} \quad \phi_z \text{ is prescribed} \tag{16}$$

$$\text{Either } Q_{xz}^2 = 0 \quad \text{or} \quad \psi_z \text{ is prescribed} \tag{17}$$

Substitution of stress resultants from Eq. (9) into Eq. (10) leads to the following form of governing differential equations in-terms of unknown displacement variables.

$$\delta u_0: \quad A_{11}\frac{d^2 u_0}{dx^2} - B_{11}\frac{d^3 w_0}{dx^3} + C_{11}\frac{d^2\phi_x}{dx^2} + D_{11}\frac{d^2\psi_x}{dx^2} + F_{13}\frac{d\phi_z}{dx} + H_{13}\frac{d\psi_z}{dx} = 0 \tag{18}$$

$$\delta w_0: \quad B_{11}\frac{d^3u_0}{dx^2}-A_{S11}\frac{d^4w_0}{dx^4}+C_{S11}\frac{d^3\phi_x}{dx^3}+D_{S11}\frac{d^3\psi_x}{dx^3}+F_{S13}\frac{d^2\phi_Z}{dx^2}+H_{S13}\frac{d^2\psi_Z}{dx^2}=-q+N_0\frac{d^2w_0}{dx^2} \tag{19}$$

$$\begin{aligned}\delta\phi_x: \quad & C_{11}\frac{d^2u_0}{dx^2}-C_{S11}\frac{d^3w_0}{dx^3}+C_{SS111}\frac{d^2\phi_x}{dx^2}+C_{SS211}\frac{d^2\psi_x}{dx^2}+F_{SS13}\frac{d\phi_Z}{dx}+H_{SS13}\frac{d\psi_Z}{dx}\\ & -F_{SS155}\left(\phi_x+\frac{d\phi_x}{dx}\right)-H_{SSS55}\left(\psi_x+\frac{d\psi_x}{dx}\right)=0\end{aligned} \tag{20}$$

$$\begin{aligned}\delta\psi_x: \quad & D_{11}\frac{d^2u_0}{dx^2}-D_{S11}\frac{d^3w_0}{dx^3}+C_{SS211}\frac{d^2\phi_x}{dx^2}+D_{SS211}\frac{d^2\psi_x}{dx^2}+F_{SSS13}\frac{d\phi_Z}{dx}+H_{SSS13}\frac{d\psi_Z}{dx}\\ & -H_{SSS55}\left(\phi_x+\frac{\partial\phi_z}{\partial x}\right)-F_{SS255}\left(\psi_x+\frac{d\psi_z}{dx}\right)=0\end{aligned} \tag{21}$$

$$\begin{aligned}\delta\phi_z: \quad & -F_{13}\frac{du_0}{dx}+F_{S13}\frac{d^2w_0}{dx^2}-F_{SS13}\frac{d\phi_x}{dx}-F_{SSS13}\frac{d\psi_x}{dx}-F_{SSS133}\phi_Z-F_{SSS233}\psi_z\\ & +F_{SS155}\left(\frac{d\phi_x}{dx}+\frac{d^2\phi_z}{dx^2}\right)+H_{SSS55}\left(\frac{d\psi_x}{dx}+\frac{d^2\psi_z}{dx^2}\right)=0\end{aligned} \tag{22}$$

$$\begin{aligned}\delta\psi_z: \quad & -H_{13}\frac{du_0}{dx}+H_{S13}\frac{d^2w_0}{dx^2}-H_{SS13}\frac{d\phi_x}{dx}-H_{SSS13}\frac{d\psi_x}{dx}+F_{SSS233}\phi_Z-H_{SSS233}\psi_z\\ & +H_{SSS55}\left(\frac{d\phi_x}{dx}+\frac{d^2\phi_z}{dx^2}\right)+F_{SS255}\left(\frac{d\psi_x}{dx}+\frac{d^2\psi_z}{dx^2}\right)=0\end{aligned} \tag{23}$$

Where

$$\left[A_{ij},B_{ij},C_{ij},D_{ij}\right]=\int_{-h/2}^{h/2}Q_{ij}(z)\left[1,z,f_1(z),f_2(z)\right]dz,$$

$$\left[A_{Sij},C_{Sij},D_{Sij},F_{Sij},H_{Sij}\right]=\int_{-h/2}^{h/2}Q_{ij}(z)z\left[z,f_1(z),f_2(z),f^{"}{}_1(z),f_2^{"}(z)\right]dz,$$

$$\left[C_{SS1ij},C_{SS2ij}\right]=\int_{-h/2}^{h/2}Q_{ij}(z)f_1(z)\left[f_1(z),f_2(z)\right]dz,$$

$$D_{SS2ij}=\int_{-h/2}^{h/2}Q_{ij}(z)f_2(z)^2dz,\quad F_{ij}=\int_{-h/2}^{h/2}Q_{ij}(z)f_1^{"}(z)dz,\quad H_{ij}=\int_{-h/2}^{h/2}Q_{ij}(z)f_2^{"}(z)dz, \tag{24}$$

$$\left[F_{SSij},H_{SSij}\right]=\int_{-h/2}^{h/2}Q_{ij}(z)f_1(z)\left[f_1^{"}(z),f_2^{"}(z)\right]dz,$$

$$\left[H_{SSSij},F_{SS2ij}\right]=\int_{-h/2}^{h/2}Q_{ij}(z)f_2^{'}(z)\left[f_1^{'}(z),f_2^{'}(z)\right]dz,$$

$$\left[F_{SSSij},H_{SSSij}\right]=\int_{-h/2}^{h/2}Q_{ij}(z)f_2(z)\left[f_1^{"}(z),f_2^{"}(z)\right]dz,$$

$$F_{SS1ij}=\int_{-h/2}^{h/2}Q_{ij}\left(z\right)f_1^{'}\left(z\right)f_1^{'}\left(z\right)dz,\quad F_{SSS1ij}=\int_{-h/2}^{h/2}Q_{ij}\left(z\right)f_1^{"}\left(z\right)f_1^{"}\left(z\right)dz,$$

$$\left[F_{SSS2ij},H_{SSS2ij}\right]=\int_{-h/2}^{h/2}Q_{ij}\left(z\right)f_2^{"}\left(z\right)\left[f_1^{"}\left(z\right),f_2^{"}\left(z\right)\right]dz,$$

2.5 Analytical Solutions

A functionally graded beam simply supported at its edges $x=0$ and $x=L$ is considered for the analytical solutions. Analytical solution for the bending analysis of simply supported functionally graded beams is obtained using Navier's solution technique. According to Navier's technique, the displacement variables are expanded into a single trigonometric series.

$$\begin{aligned}&u_0=\sum_{m=1}^{\infty}u_m\cos\alpha x,\quad w_0=\sum_{m=1}^{\infty}w_m\sin\alpha x,\quad \phi_x=\sum_{m=1}^{\infty}\phi_{xm}\cos\alpha x,\\&\psi_x=\sum_{m=1}^{\infty}\psi_{xm}\cos\alpha x,\quad \phi_z=\sum_{m=1}^{\infty}\phi_{zm}\sin\alpha x,\quad \psi_z=\sum_{m=1}^{\infty}\psi_{zm}\sin\alpha x\end{aligned}\tag{25}$$

where $u_m, w_m, \phi_{xm}, \psi_{xm}, \phi_{zm}, \psi_{zm}$ are unknown coefficients and $\alpha=m\pi/L$. The transverse load $q(x)$ acting on the top surface of the beam is also expanded in a single trigonometric series.

$$q\left(x\right)=\sum_{m=1}^{\infty}q_m\sin\alpha x\tag{26}$$

Where

$$\begin{cases}q_m=q_0 & \left(\text{Sinusoidal load}\right)\\ q_m=\dfrac{4q_0}{m\pi} & \left(\text{Uniformly distributed load}\right)\end{cases}\tag{27}$$

Substituting the trigonometric form of $u_0,w_0,\phi_x,\psi_x,\phi_z,\psi_z$ and $q(x)$ from Eqs. (25)-(27) into governing equations (18)-(23), the analytical solutions can be obtained from the following equation.

$$\left[K\right]\left\{\Delta\right\}=\left\{f\right\}\tag{28}$$

where $[K]$ is the stiffness matrix, $\{f\}$ is the force vector and $\{\Delta\}$ is the vector of unknowns coefficients. The elements of the $[K],\{\Delta\}$ and $\{f\}$ are as follows,

$$\begin{aligned}&K_{11}=-A_{11}\alpha^2,K_{12}=B_{11}\alpha^3,K_{13}=-C_{11}\alpha^2,K_{14}=-D_{11}\alpha^2,K_{15}=F_{13}\alpha,K_{16}=H_{13}\alpha,\\&K_{21}=B_{11}\alpha^3,\ K_{22}=-A_{S11}\alpha^4,K_{23}=C_{S11}\alpha^3,K_{24}=D_{S11}\alpha^3,K_{25}=-F_{S13}\alpha^2,K_{26}=-H_{S13}\alpha^2\\&K_{31}=-C_{11}\alpha^2,\ K_{32}=C_{S11}\alpha^3,\ K_{33}=-(C_{SS111}\alpha^2+F_{SS155}),\quad K_{34}=-(C_{SS211}\alpha^2+H_{SSS55}),\\&K_{35}=(F_{SS13}-F_{SS155})\alpha,K_{36}=(H_{SS13}-H_{SSS55})\alpha,K_{41}=-D_{11}\alpha^2,\ K_{42}=D_{S11}\alpha^3,\\&K_{43}=-(C_{SS211}\alpha^2+H_{SSS55}),K_{44}=-(D_{SS211}\alpha^2+F_{SS255}),K_{45}=(F_{SSS13}-H_{SSS55})\alpha,\\&K_{46}=(H_{SSS13}-F_{SS255})\alpha,\quad K_{51}=F_{13}\alpha,K_{52}=-F_{S13}\alpha^2,K_{53}=(F_{SS13}-F_{SS155})\alpha,\end{aligned}\tag{29}$$

$$K_{54} = (F_{SSS13} - H_{SSS55})\alpha,\ K_{55} = -(F_{SS155}\alpha^2 + F_{SSS133}),$$
$$K_{56} = -(H_{SSS155}\alpha^2 + F_{SSS233}), K_{61} = H_{13}\alpha,\ K_{62} = -H_{S13}\alpha^2,\ K_{63} = (H_{SS13} - H_{SSS55})\alpha,$$
$$K_{64} = (H_{SSS13} - F_{SS255})\alpha,\ K_{65} = -(H_{SSS55}\alpha^2 + F_{SSS233}),\ K_{66} = -(F_{SS255}\alpha^2 + H_{SSS233})$$
$$\{\Delta\} = \{u_m, w_m, \phi_{xm}, \psi_{xm}, \phi_{zm}, \psi_{zm}\}^T \quad \text{and} \quad \{f\} = \{0 \quad 0 \quad q_m \quad 0 \quad 0 \quad 0\}^T$$

3 NUMERICAL RESULTS AND DISCUSSION

In the section static bending and elastic buckling problems are presented and discussed to verify the accuracy of the present theory. For numerical results, the P-FGM beam made of metal (Aluminum: E_m= 70 GPa and μ_m= 0.3) and ceramic (Alumina: E_c= 380GPa, μ_c= 0.3) is considered. The material properties of P-FGM beam varying continuously in the thickness direction according to the power-law distribution. Displacements and stresses are presented in the following non-dimensional form

$$\bar{w}, \bar{w}_b, \bar{w}_s\left(\frac{L}{2}, 0\right) = \frac{100E_m h^3}{q_0 L^4}(w, w_b, w_s),\quad \bar{u}\left(0, -\frac{h}{2}\right) = \frac{100E_m h^3 u}{q_0 L^4},$$
$$\bar{\sigma}_x\left(\frac{L}{2}, \frac{h}{2}\right) = \frac{h\sigma_x}{q_0 L},\quad \bar{\tau}_{xz}(0,0) = \frac{h\tau_{xz}}{q_0 L},\qquad \bar{N}_{cr} = \frac{12N_0 L^2}{E_m h^3} \tag{30}$$

3.1 Bending of P-FGM Beam

Table 1 shows non-dimensional bending ($\bar{w}_b$) and shear components ($\bar{w}_s$) of transverse displacement ($\bar{w}$) for FG beams subjected to a sinusoidal load. The numerical results are obtained for various values of the power law index and aspect ratios. From Table 1 it reveals that shear component of transverse displacement is decreases with increase in aspect ratio. This is in fact due to, shear deformation is more pronounced in thick beams than the slender beams. Also, the transverse displacement is increases with an increase in power law index which is due to decrease in stiffness of the beam.

Table 2 shows a comparison of maximum non-dimensional displacements and stresses of FG beam subjected to a sinusoidal load for various values of the power law index (P) and (L/h) ratio 5. Present results are compared with the parabolic shear deformation theory of Reddy (1984), a unified shear deformation theory of Sayyad and Ghugal (2017b), first order shear deformation of Timoshenko (1921) and classical beam theory of Bernoulli-Euler. The axial and transverse displacements obtained by using the present theory are in close agreement with those obtained by using other refined theories. It is observed that displacements are increased with an increase in power law index. The displacements are maximum when $p = \infty$ (fully metal beam) and minimum when $p = 0$ (fully ceramic beam). This is due to the fact that an increase in the power law index increases the flexibility of FG beam. Classical beam theory underestimates the displacements compared to first order and higher order theories due to neglect of transverse shear deformation effect. Figure 3 shows through the thickness distribution of axial stress, whereas variation of transverse displacement for various aspect ratios is plotted in Figure 4. The variation of axial stress through the thickness of the beam is plotted in Figure 5, which reveals that the axial stress is

compressive in nature when the beam is of fully metal and tensile when it is of fully ceramic. The variation of axial stress is non-linear through the thickness for $P = 1, 5, 10$ and linear for $P = 0$ and ∞. It is also pointed out that the axial stresses in metal and ceramic beams are identical. The Fig. 6 shows through the thickness distribution of transverse shear stress, which is zero at top and bottom surfaces, but not maximum at the center of the cross-section due to continuous variation of material properties through the thickness of the beam.

L/h	P	$\overline{w}_b$	$\overline{w}_s$	$\overline{w} = \overline{w}_b + \overline{w}_s$
5	0(Ceramic)	2.4590	0.0289	2.4879
	1	4.7964	0.0488	4.8452
	2	6.1203	0.0377	6.1580
	5	7.5004	0.0448	7.5452
	10	8.4273	0.0830	8.5103
	∞ (Metal)	13.310	0.1568	13.467
10	0 (Ceramic)	2.3171	0.0810	2.3981
	1	4.5640	0.0137	4.5777
	2	5.7659	0.0103	5.7762
	5	6.8961	0.0120	6.9082
	10	7.7207	0.0241	7.7448
	∞ (Metal)	12.578	0.0441	12.622
100	0 (Ceramic)	2.2712	0.0008	2.2719
	1	4.4888	0.0016	4.4904
	2	5.6497	0.0010	5.6507
	5	6.6969	0.0016	6.6985
	10	7.4900	0.0018	7.4918
	∞ (Metal)	12.329	0.0004	12.329

Table 1: Non–dimensional bending and shear components of transverse displacement of P-FGM beams subjected to sinusoidal load.

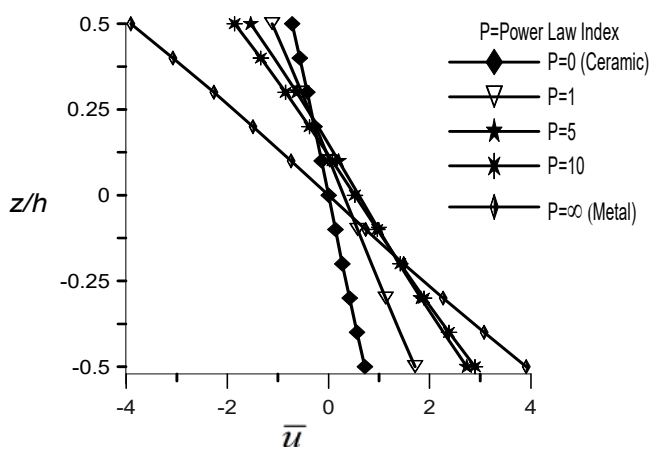

Figure 3: Through thickness variation of non-dimensional axial displacement ($\overline{u}$) of simply supported P-FGM beam subjected to sinusoidal load (L/h=5).

P	Theory	Model	$\overline{u}$ (-h/2)	$\overline{w}$ (0)	$\overline{\sigma}_x$ (h/2)	$\overline{\tau}_{xz}$ (0)
0 (Ceramic)	Present ($\varepsilon_z \neq 0$)	FOSNDT	0.7202	2.4808	3.0999	0.5474
	Reddy (1984) ($\varepsilon_z = 0$)	PSDT	0.7251	2.5020	3.0916	0.4769
	Sayyad and Ghugal (2017b) ($\varepsilon_z = 0$)	TSDT	0.7259	2.5016	3.0949	0.4920
	Sayyad and Ghugal (2017b) ($\varepsilon_z = 0$)	HSDT	0.7247	2.5003	3.0899	0.4739
	Sayyad and Ghugal (2017b) ($\varepsilon_z = 0$)	ESDT	0.7280	2.4974	3.1039	0.4871
	Timoshenko (1921) ($\varepsilon_z = 0$)	FSDT	0.7129	2.5023	3.0396	0.3183
	Bernoulli-Euler ($\varepsilon_z = 0$)	CBT	0.7129	2.2693	3.0396	---
1	Present ($\varepsilon_z \neq 0$)	FOSNDT	1.7131	4.8452	4.7667	0.5225
	Reddy [1984] ($\varepsilon_z = 0$)	PSDT	1.7793	4.9458	4.7856	0.5243
	Sayyad and Ghugal (2017b) ($\varepsilon_z = 0$)	TSDT	1.7806	4.9451	4.7912	0.5331
	Sayyad and Ghugal (2017b) ($\varepsilon_z = 0$)	HSDT	1.7517	4.9257	4.7165	0.6025
	Sayyad and Ghugal (2017b) ($\varepsilon_z = 0$)	ESDT	1.7819	4.9432	4.7964	0.5430
	Timoshenko (1921) ($\varepsilon_z = 0$)	FSDT	1.7588	4.8807	4.6979	0.5376
	Bernoulli-Euler ($\varepsilon_z = 0$)	CBT	1.7588	4.5528	4.6979	---
5	Present ($\varepsilon_z \neq 0$)	Present	2.7339	7.5452	6.3352	0.5026
	Reddy (1984) ($\varepsilon_z = 0$)	PSDT	2.8644	7.7723	6.6057	0.5314
	Sayyad and Ghugal (2017b) ($\varepsilon_z = 0$)	TSDT	2.8671	7.7792	6.6172	0.5144
	Sayyad and Ghugal (2017b) ($\varepsilon_z = 0$)	HSDT	2.8641	7.7715	6.6047	0.5332
	Sayyad and Ghugal (2017b) ($\varepsilon_z = 0$)	ESDT	2.8697	7.7830	6.6281	0.5022
	Timoshenko (1921) ($\varepsilon_z = 0$)	FSDT	2.8250	7.5056	6.4382	0.9942
	Bernoulli-Euler ($\varepsilon_z = 0$)	CBT	2.8250	6.8994	6.4382	---
10	Present ($\varepsilon_z \neq 0$)	FOSNDT	2.8969	8.5103	7.8979	0.4431
	Reddy (1984) ($\varepsilon_z = 0$)	PSDT	2.9989	8.6530	7.9080	0.4226
	Sayyad and Ghugal (2017b) ($\varepsilon_z = 0$)	TSDT	3.0022	8.6561	7.9195	0.4392
	Sayyad and Ghugal (2017b) ($\varepsilon_z = 0$)	HSDT	2.9986	8.6527	7.9070	0.4211
	Sayyad and Ghugal (2017b) ($\varepsilon_z = 0$)	ESDT	3.0054	8.6547	7.9301	0.4558
	Timoshenko (1921) ($\varepsilon_z = 0$)	FSDT	2.9488	8.3259	7.7189	1.2320
	Bernoulli-Euler ($\varepsilon_z = 0$)	CBT	2.9488	7.5746	7.7189	---
∞ (Metal)	Present ($\varepsilon_z \neq 0$)	FOSNDT	3.9097	13.505	3.0999	0.5474
	Reddy (1984) ($\varepsilon_z = 0$)	PSDT	3.9363	13.582	3.0916	0.4769
	Sayyad and Ghugal (2017b) ($\varepsilon_z = 0$)	ESDT	3.9444	13.574	3.0980	0.5072
	Timoshenko (1921) ($\varepsilon_z = 0$)	FSDT	3.8702	12.552	3.0396	0.3183
	Bernoulli-Euler ($\varepsilon_z = 0$)	CBT	3.8702	12.319	3.0396	----

Table 2: Comparison of axial displacement $\overline{u}$ at ($x = 0$), transverse deflection $\overline{w}$ at ($x = L/2$), normal stress $\overline{\sigma}_x$ at ($x = L/2$) and transverse shear stress $\overline{\tau}_{xz}$ at ($x = 0$) in P-FGM beams ($L = 5h$) subjected to sinusoidal load.

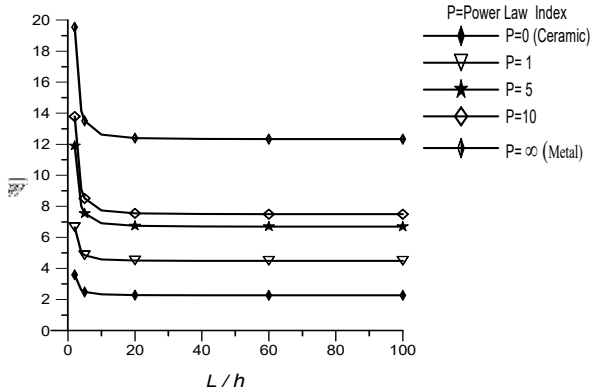

Figure 4: Variation of non-dimensional transverse displacement ($\overline{w}$) of simply supported P-FGM beam subjected to sinusoidal load using various aspect ratios.

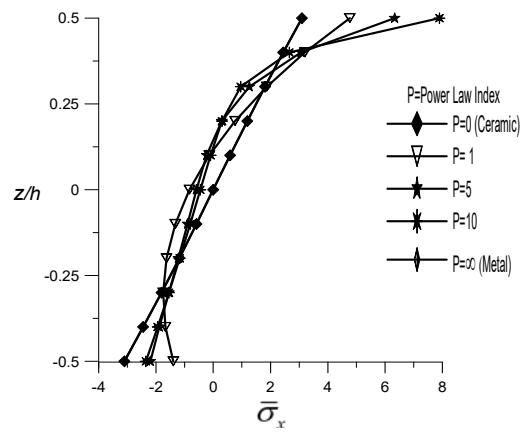

Figure 5: Through thickness variation of non-dimensional bending stress ($\overline{\sigma}_x$) of simply supported P-FGM beam subjected to sinusoidal load (L/h=5).

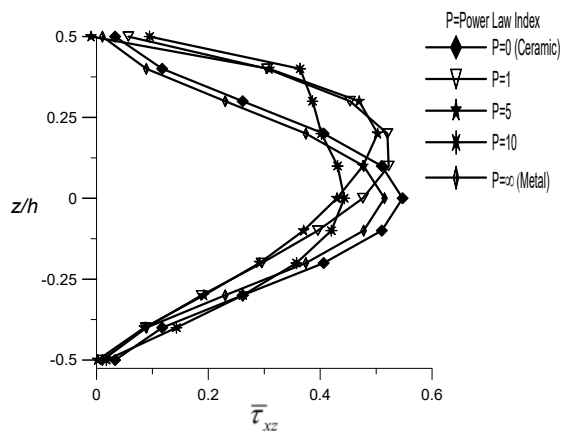

Figure 6: Through thickness variation of non-dimensional transverse shear stress ($\overline{\tau}_{xz}$) of simply supported functionally graded beam subjected to sinusoidal load (L/h=5).

Comparison of maximum non-dimensional displacements and stresses of FG beam subjected to a uniformly distributed load for various values of the power law index is presented in Table 3. The present results are compared with those obtained by using other higher order theories. It is observed that displacements and stresses are increased with an increase in power law index. This is due to the fact that an increase of the power law index increases the flexibility of FG beam. Displacements and stresses predicted by using the present theory are in excellent agreement with those obtained by using other higher order beam theories. Through thickness distributions of axial displacement, bending stress and transverse shear stress are plotted in Figures 7, 9 and 10 respectively, whereas variation of transverse displacement with respect to L/h ratio is shown in Fig. 8.

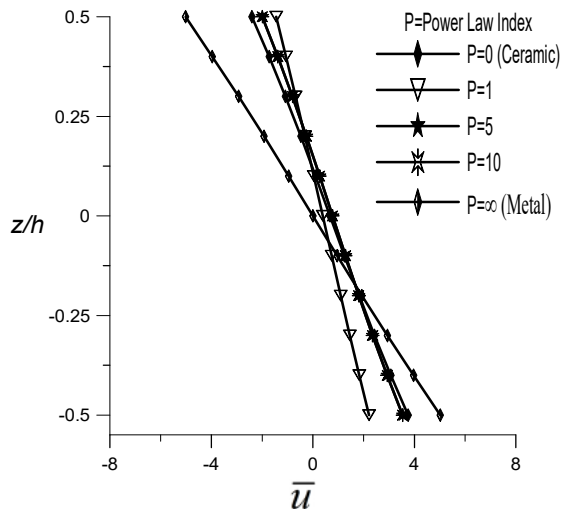

Figure 7: Through thickness variation of non-dimensional axial displacement ($\overline{u}$) of simply supported P-FGM beam subjected to uniformly distributed load (L/h=5).

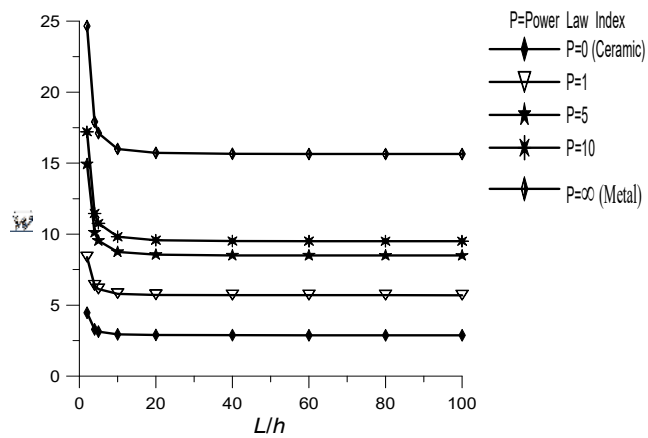

Figure 8: Variation of non-dimensional transverse displacement ($\overline{w}$) of simply P-FGM beam subjected to uniformly distributed load using various aspect ratios.

P	Theory	Model	$\overline{u}$ (-h/2)	$\overline{w}$ (0)	$\overline{\sigma}_x$ (h/2)	$\overline{\tau}_{xz}$ (0)
0 (Ceramic)	Present $(\varepsilon_z \neq 0)$	FOSNDT	0.9260	3.1395	3.7931	0.7325
	Reddy (1984) $(\varepsilon_z = 0)$	PSDT	0.9397	3.1654	3.8028	0.7305
	Sayyad and Ghugal (2017b) $(\varepsilon_z = 0)$	TSDT	0.9409	3.1649	3.8061	0.7524
	Sayyad and Ghugal (2017b) $(\varepsilon_z = 0)$	HSDT	0.9391	3.1633	3.8010	0.7246
	Sayyad and Ghugal (2017b) $(\varepsilon_z = 0)$	ESDT	0.9441	3.1598	3.8152	0.7438
	Timoshenko (1921) $(\varepsilon_z = 0)$	FSDT	0.9210	3.1657	3.7501	0.4922
	Bernoulli-Euler $(\varepsilon_z = 0)$	CBT	0.9210	2.8783	3.7501	----
1	Present $(\varepsilon_z \neq 0)$	FOSNDT	2.2161	6.1335	5.8674	0.8024
	Reddy (1984) $(\varepsilon_z = 0)$	PSDT	2.3037	6.2594	5.8850	0.8031
	Sayyad and Ghugal (2017b) $(\varepsilon_z = 0)$	TSDT	2.3036	6.2586	5.8906	0.8152
	Sayyad and Ghugal (2017b) $(\varepsilon_z = 0)$	HSDT	2.2618	6.2361	5.8150	0.8811
	Sayyad and Ghugal (2017b) $(\varepsilon_z = 0)$	ESDT	2.3074	6.2563	5.8958	0.8288
	Timoshenko (1921) $(\varepsilon_z = 0)$	FSDT	2.2722	6.1790	5.7960	0.8313
	Bernoulli-Euler $(\varepsilon_z = 0)$	CBT	2.2722	5.7746	5.7960	----
5	Present $(\varepsilon_z \neq 0)$	Present	3.5388	9.5411	7.7638	0.7709
	Reddy (1984) $(\varepsilon_z = 0)$	PSDT	3.7098	9.8281	8.1127	0.8114
	Sayyad and Ghugal (2017b) $(\varepsilon_z = 0)$	TSDT	3.7138	9.8367	8.1242	0.7836
	Sayyad and Ghugal (2017b) $(\varepsilon_z = 0)$	HSDT	3.7095	9.8271	8.1117	0.8144
	Sayyad and Ghugal (2017b) $(\varepsilon_z = 0)$	ESDT	3.7176	9.8414	8.1351	0.7633
	Timoshenko (1921) $(\varepsilon_z = 0)$	FSDT	3.6496	9.4987	7.9430	1.5373
	Bernoulli-Euler $(\varepsilon_z = 0)$	CBT	3.6496	8.7508	7.9430	----
10	Present $(\varepsilon_z \neq 0)$	FOSNDT	3.7514	10.760	9.7170	0.6596
	Reddy (1984) $(\varepsilon_z = 0)$	PSDT	3.8861	10.938	9.7146	0.6451
	Sayyad and Ghugal (2017b) $(\varepsilon_z = 0)$	TSDT	3.8910	10.942	9.7261	0.6691
	Sayyad and Ghugal (2017b) $(\varepsilon_z = 0)$	HSDT	3.8857	10.937	9.7137	0.6432
	Sayyad and Ghugal (2017b) $(\varepsilon_z = 0)$	ESDT	3.8956	10.940	9.7367	0.6929
	Timoshenko (1921) $(\varepsilon_z = 0)$	FSDT	3.8096	10.534	9.5231	1.9050
	Bernoulli-Euler $(\varepsilon_z = 0)$	CBT	1.8096	9.6072	9.5231	----
∞ (Metal)	Present $(\varepsilon_z \neq 0)$	FOSNDT	5.0210	17.110	3.7984	0.8232
	Reddy (1984) $(\varepsilon_z = 0)$	PSDT	5.1012	17.183	3.8028	0.7305
	Sayyad and Ghugal (2017b) $(\varepsilon_z = 0)$	ESDT	5.1133	17.173	3.8084	0.7741
	Timoshenko (1921) $(\varepsilon_z = 0)$	FSDT	5.0000	15.912	3.7501	0.4922
	Bernoulli-Euler $(\varepsilon_z = 0)$	CBT	5.0000	15.625	3.7501	---

Table 3: Comparison of axial displacement $\overline{u}$ at $(x = 0)$, transverse deflection $\overline{w}$ at $(x = L/2)$, normal stress $\overline{\sigma}_x$ at $(x = L/2)$ and transverse shear stress $\overline{\tau}_{xz}$ at $(x = 0)$ in P-FGM beams $(L = 5h)$ subjected to uniformly distributed load.

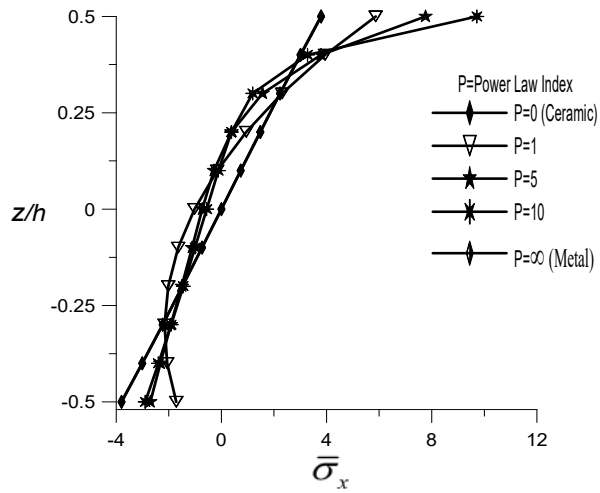

Figure 9: Through thickness variation of non-dimensional bending stress ($\overline{\sigma}_x$) of simply supported functionally graded beam subjected to uniformly distributed load (L/h=5).

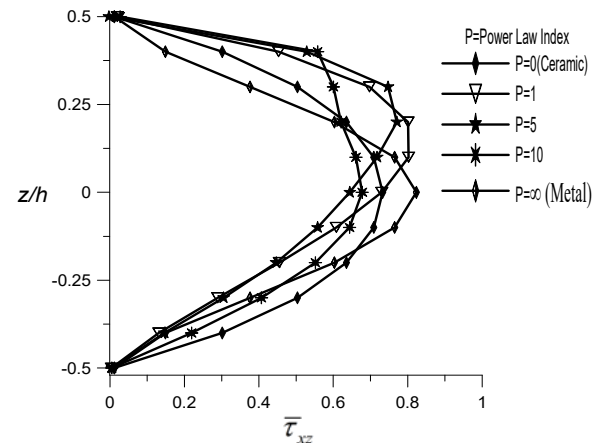

Figure 10: Through thickness variation of non-dimensional transverse shear stress ($\overline{\tau}_{xz}$) of simply supported functionally graded beam subjected to uniformly distributed load (L/h=5).

3.2 Buckling of P-FGM beam

In this section, elastic buckling response of functionally P-FGM beam is investigated using the present theory. Non-dimensional critical buckling load obtained using the present theory is compared with that of other higher order shear deformation theories and tabulated in Table 4. From Table 4, it is point out that the critical buckling load decreases with increase in power law index. This is due to the fact that an increase of the power law index decreases the stiffness of P-FGM beam (see Figure 11). Present results are compared with those presented by Li and Batra (2013), Nguyen et al. (2013) and Vo et al. (2014). The examination of Table 4 reveals that the present results are in excellent agreement with those presented by other researchers.

			Power law index					
L/h	Theory	Model	0(Ceramic)	1	2	5	10	∞ (Metal)
5	Present ($\varepsilon_z \neq 0$)	FOSNDT	49.4448	25.3494	19.8659	16.2105	14.4279	9.1082
	Li and Batra (2013)	PSDT	48.8350	24.6870	19.2450	16.0240	14.4270	----
	Nguyen et al.(2013)	FSDT	48.8350	24.6870	19.2450	16.0240	14.4270	----
	Vo et al.(2014)	HSDT	48.8372	24.6898	19.2479	16.0263	14.4286	----
	Vo et al. (2014)	FSDT	48.8401	24.6911	19.1605	15.7400	14.1468	----
10	Present ($\varepsilon_z \neq 0$)	FOSNDT	52.4734	26.6399	21.0870	17.6309	15.7480	9.6662
	Li and Batra (2013)	PSDT	52.3090	26.1710	20.4160	17.1920	15.6120	----
	Nguyen et al.(2013)	FSDT	52.3090	26.1710	20.4160	17.1940	15.6120	----
	Vo et al.(2014)	HSDT	52.3085	26.1728	20.4187	17.1959	15.6134	----
	Vo et al (2014)	FSDT	52.3082	26.1727	20.3963	17.1118	15.5291	----

Table 4: Comparison of Non-dimensional critical buckling load (F_{cr}) o simply supported P-FGM beams with various values of power law index (P).

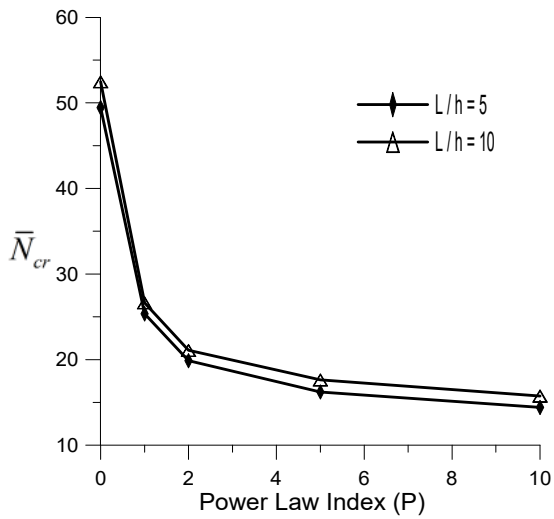

Figure 11: The variation of non-dimensional critical buckling load with respect to the power law index for simply supported P-FGM beam.

4 CONCLUSIONS

A fifth-order shear and normal deformation theory is developed in the present study for the static bending and elastic buckling of FG beam. The theory shows fifth-order variation of axial displacement and a fourth order variation of transverse displacement. The theory satisfies the traction free boundary conditions at top and bottom surfaces of the beam without using problem dependent shear correction factor. Variationally consistent governing differential equations and associated boundary conditions are obtained using the principle of virtual work. Analytical solutions are obtained for a simply supported boundary condition using Navier's technique. Effects of transverse shear and normal deformations on the bending of FG beams are investigated. From the numerical results and discussion following conclusions are made.

1) Since shear deformation is more pronounced in thick beam, shear component of transverse displacement decreases with increase in aspect ratio.
2) An Increase in the power law index decreases the stiffness of the beam. Therefore, displacements are increased with an increase in the power law index.
3) The variation of axial stress is non-linear through the thickness for $P = 1, 5, 10$ and linear for $P = 0$ and ∞. Axial stress is compressive in nature when the beam is of fully metal and tensile when it is of fully ceramic.
4) The transverse shear stress is not maximum at the center of the cross-section due to continuous variation of material properties through the thickness of the beam.
5) From the buckling response of the functionally graded beam, it is observed that the critical buckling load decreases with an increase in power law index and increases with increase in L/h ratio.

References

Benatta, M. A., Mechab, I., Tounsi, A., Bedia, E. A. A. (2008). Static analysis of functionally graded short beams including warping and shear deformation effects. Computational Material Science 44:765–773.

Birman, V., and Byrd, L.W. (2006). Functionally graded stitched laminates: illustration on the example of a double cantilever beam. ASCE Journal of Aerospace Enginering19:217-226.

Birman, V., and Byrd, L.W. (2007). Modeling and analysis offunctionally graded materials and structures. ASME Applied Mechanics Review 60:195-216.

Bourada M., Kaci A., Houari M. S. A., and Tounsi A. (2015). A new simple shear and normal deformations theory for functionally graded beams. Steel and Composite Structures 18:409-423.

Carrera, E. (2005). Transverse normal strain effects on termal stress analysis of homogeneous and layered plates. AIAA Journal 43(10):2232-2242.

Carrera, E., Giunta, G., and Petrolo, M. (2011). Beam Structures: Classical and Advanced TheoriesJohn Wiley & Sons Ltd U.K.

Chu, P., Li, X. F., Wu, J. X., Lee, K. Y. (2015). Two-dimensional elasticity solution of elastic strips and beams made of functionally graded materials under tension and bending. Acta Meccanica226:2235–2253.

Daouadji, T. H., Henni, A.H.,Tounsi, A, Bedia E. A. A. (2013). Elasticity solution of a cantilever functionally graded beam. Applied Composite Material 20:1–15.

Giunta, G., Belouettar, S., and Carrera, E. (2010). Analysis of FGM beams by means of classical and advanced theories. Mechanics of Advanced Materials and Structures 17(8):622-635.

Giunta, G., Crisafulli, D., Belouettar, S., Carrera, E. (2011). Hierarchical theories for the free vibration analysis of functionally graded beams. Composite Structures 94(1):68-74.

Jha, D. K., Kant, T., and Singh, R. K. (2013). A critical review of recent research on functionally graded plates. Composite Structures 96:833–849.

Koizumi, M. (1993). The concept of FGM. Ceramic Transactions. Functionally Gradient Materials 34:3-10.

Koizumi, M. (1997). FGM activities in Japan. Composite Part B 28:1–4.

Li, S.R., and Batra, R.C. (2013). Relations between buckling loads of functionally graded Timoshenko and homogeneous Euler–Bernoulli beams. Composite Structures 95:5–9.

Li, X. F.,Wang, B. L., and Han J. C. (2010). A higher-order theory for static and dynamic analyses of functionally graded beams. Archives of Applied Mechanics 80:1197–1212.

Muller, E., Drasar, C., Schilz, J., Kaysser, W. A. (2003). Functionally graded materials for sensor and energy applications. Material Science and Engineering A362:17–39.

Nguyen, T.K., Vo, T.P., Thai, H.T. (2013). Static and free vibration of axially loaded functionally gradedbeams based on the first-order shear deformation theory. Composite Part B 55:147–157.

Pendhari, S. S., Kant, T., Desai, Y. M., Subbaiah, C. V. (2010). On deformation of functionally graded narrow beams under transverse loads. International Journal of Mechanics and Material Design 6:269–282.

Rasheedat, M. M., Esther, T. A., Muku, S., and Sisa, P. (2012). Functionally Graded Material: An Overview. Procedding of World Congress on Engineering3:1-5.

Reddy, J.N. (1984).A simple higher order theory for laminated composite plates. ASME Journal of Applied Mechanics51:745-752.

Sankar, B. V. (2001).An elasticity solution for functionally graded beams. Composite Scienceand Technology 61:689–696.

Sayyad, A. S., and Ghugal, Y. M. (2015). On the free vibration analysis of laminated composite and sandwich plates: A review of recent literature with some numerical results. Composite Structures 129:177–201.

Sayyad, A. S., and Ghugal, Y. M. (2017a). Bending, buckling and free vibration of laminated composite and sandwich beams: A critical rivew of literature. Composite Structures 171:486–504.

Sayyad, A. S., and Ghugal, Y. M. (2017b). A unified shear deformation theory for the bending of isotropic, functionally graded, laminated and sandwich beams and plates. International Journal of Applied Mechanics 9(1): 1-36.

Simsek, M. (2016). Buckling of Timoshenko beams composed of two-dimensional functionally graded material 2D-FGM having different boundary conditions. Composite Structures149:304-331.

Swaminathan, K., Naveenkumar, D. T., Zenkour, A. M., and Carrera E. (2014). Stress, vibration and buckling analyses of FGM plates-A state-of-the-art review. Composite Structures 120:10-31.

Thai, H. T., and Vo, T. P. (2012). Bending and free vibration of functionally graded beams using various higher-order shear deformation beam theories. International Journal of Mechanical Sciences 62:57–66.

Timoshenko, S. P. (1921). On the correction for shear of the differential equation for the transverse vibration of prismatic bars. Philosophical Magazine 41:742-746.

Vo, T.P., Thai, H.T., Nguyen, T.K., Inam, F. (2014). Static and vibration analysis of functionally graded beams using refined shear deformation theory. Meccanica 49:155–168.

Zhong, Z., and Yu, T. (2007). Analytical solution of a cantilever functionally graded beam. Composite Science and Technology 67:481–488.